THE BELL SYSTEM

TECHNICAL JOURNAL

VOLUME XLII JANUARY 1963 NUMBER 1

A Method for Predicting Interchannel Modulation due to Multipath Propagation in FM and PM Tropospheric Radio Systems*

By C. D. BEACH and J. M. TRECKER

(Manuscript received August 7, 1962)

This paper describes a method for predicting the magnitude of interchannel modulation due to multipath propagation on angle-modulated tropospheric scatter radio systems. Values of signal-to-intermodulation ratio, S/I, are calculated for various pairs of signal reflections in the troposphere, taking into account the base bandwidth and frequency deviation of the system, the antenna patterns, the path geometry, and climatic conditions during the "worst month" of propagation. The lowest value of S/I (worst intermodulation) computed for such pairs of signal reflections is then corrected empirically to account for multiple reflections. The result represents the median value of S/I expected during the worst month of transmission on a specified path.

The method yields results that, when compared to measured results from four widely different paths normalized to worst-month conditions, have a standard error of estimate of about 2.6 db.

TABLE OF CONTENTS

* The experimental data discussed in this paper were obtained from tests carried out under Contract AF33(600)-36661 with the U.S. Air Force, Air Material Command.

I. INTRODUCTION

Various theories have been proposed to explain the mechanism by which energy radiated from a transmitting antenna is reflected or refracted in the atmosphere and ultimately arrives at a receiving antenna beyond the horizon.[1,2,3] Apart from the merits of any particular theory of propagation, the geometry of a typical over-the-horizon, or "tropospheric scatter," path suggests an inherent multipath transmission problem. As illustrated by Fig. 1, components of signal reflected to the receiving antenna from successively higher points in the atmosphere are delayed by increasing amounts behind the earliest arriving component.

When such time-delayed RF signals — called echoes henceforth — are demodulated by an FM or PM receiver, they are converted into energy at undesired regions of the baseband. In a frequency-division multiplexed, multi-channel voice system, this undesired energy is commonly called "interchannel modulation," or simply "intermodulation." It adds to other distortion energy generated by equipment nonlinearities and to the ever-present white noise, to produce the total background of noise faced by the desired speech signal. Whether or not "path intermodulation" noise is objectionable in a given system depends on its magnitude relative to these other components of noise.

The general theory of interchannel modulation due to transmission echoes in angle-modulated systems has been treated by Bennett, Curtis,

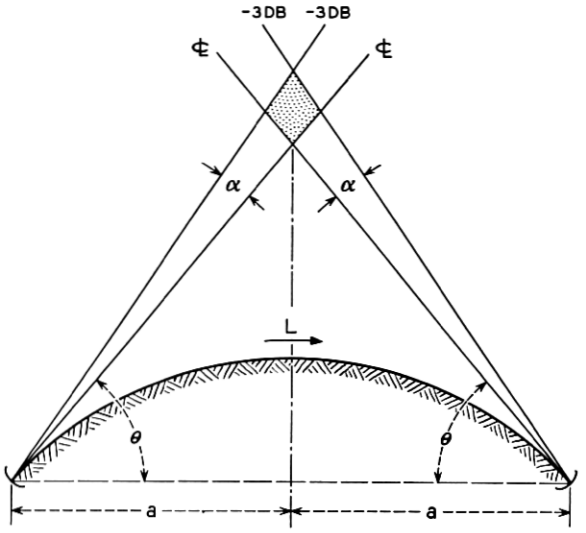

Fig. 1 — Symmetrical tropospheric scatter path.

and Rice.[4] The objective of the present paper is to outline a method for predicting the magnitude of intermodulation due to echoes in tropospheric scatter radio systems, making use of the intermodulation theory developed in Ref. 4 and the reflection theory of tropospheric propagation given in Ref. 3.

The first step in the method, following specification of a suitable model, involves calculation of the relative amplitudes of signal echoes received from various angles of elevation above the horizon. The corresponding time delays of these echoes are then calculated, relative to the signal arriving via the antenna beam axes, or "centerline" path.

Next, signal-to-intermodulation ratios are determined for selected combinations of echo amplitude and corresponding time delay, radio system base bandwidth, and frequency deviation.

These initial, primarily analytical, steps provide an indication of the magnitude of intermodulation which would be generated by single echoes in an angle-modulated system without diversity. The results postulate a so-called "worst echo"; that is, an echo having a combination of amplitude and time delay that produces more interchannel interference than any other combination.

In calculating the values of echo amplitude and time delay, the meteorological conditions of the path are assumed to be the median values during the worst month of propagation. Thus, the calculated in-

termodulation represents the median value for a single worst echo during the worst month of transmission on the given path.

From this point, the method becomes empirical in accounting for variations in the calculated median value of intermodulation as propagation conditions change, and in accounting for the effects of multiple echoes and diversity reception. Satisfactory analytical methods of handling these factors have been elusive, to say the least. However, experimental results have provided encouraging means of estimating correction factors for their effects, and these corrections are discussed.

II. MODEL OF TROPOSPHERIC SCATTER PATH

The typical geometry of a tropospheric scatter path is illustrated in Fig. 1, showing two narrow antenna beams intersecting to form a "common volume." The lower edges of the pattern represent the beam centerlines; each is pointed toward the horizon on the azimuth of the other antenna. The upper edges of the patterns are arbitrarily chosen to correspond to some value of antenna gain — e.g., 3 db — less than the centerline maximum. Throughout this paper, the antenna pattern above the centerline is assumed to be the same as half the free-space pattern.

2.1 *Reflection Theory*

The reflection theory of beyond-the-horizon transmission proposed by Friis, Crawford, and Hogg[3] has been found to yield estimates of received power which are in good agreement with reported experimental data. The expression for received power proposed by this theory will be adopted in the present model for use later in deriving an expression for echo amplitude.

Assuming identical transmitting and receiving antennas, and "intermediate-size" reflecting layers,* the received power in a system with symmetrical geometry as in Fig. 1 is given by:

$$P_r = P_t \frac{M}{3} \frac{\lambda^3}{\alpha^3} \frac{1}{\theta^5 a^2} \frac{1}{\left(2 + \frac{\alpha}{\theta}\right)} f\left(\frac{\alpha}{\theta}\right) \tag{1}$$

where

P_t = transmitted power, in watts,

M = a constant of the path proportional to the number of reflecting

* Ref. 3 proposes somewhat different expressions for the cases of large, intermediate, and small reflecting layers, where the dimensions are defined in terms of wavelength and Fresnel zones. All three may be present on a given path at various times, but intermediate-sized layers are probably most prevalent.

layers and the squares of path length, reflecting layer length, and change in gradient of refractive index at the bottom of the common volume,

λ = wavelength, meters,

α = antenna beamwidth to the half-power points, radians,

θ = angle between a chord joining the ends of the path and the axis of the antenna beam, radians,

a = half the length of the chord between the ends of the path, in meters. For practical paths, this can also be taken as half the ground distance between terminals,

and

$$f\left(\frac{\alpha}{\theta}\right) = 1 + \frac{1}{\left[1 + \frac{\alpha}{\theta}\right]^4} - \frac{1}{8}\left[\frac{2 + \frac{\alpha}{\theta}}{1 + \frac{\alpha}{\theta}}\right]^4.$$

Equation (1) indicates that the received power is critically dependent on the angle θ, and it will become apparent later that path intermodulation also depends heavily on this parameter. Therefore, it is of interest to consider those factors which influence the value of θ on a path of given length. These factors — atmospheric refractivity, unequal elevation of antenna sites, and nonhorizontal antenna take-off angles — will now be discussed.

2.2 *Effect of Refractivity on Angle* θ

As is customary in many radio problems where the transmitted signal is refracted by the atmosphere, the lines of propagation in Fig. 1 have been drawn straight over an earth having an effective radius greater than the true earth's radius. The symmetrical path is then defined completely by the path length L (or alternatively, the chord length $2a$) and the angle θ between the chord and the earth-tangent ray at either end of the path.

The value of θ which gives the correct altitude of intersection for horizontally directed antenna beams, allowing for refractive bending, is

$$\theta = \frac{L}{2R} = \frac{L}{2R_oK} \tag{2}$$

where R is the effective earth's radius, R_o is the true earth's radius (3960 statute miles), and K is a constant.

The value $K = \frac{4}{3}$ is used in many radio applications. It has been found in the present work that better results are obtained if the value of K is

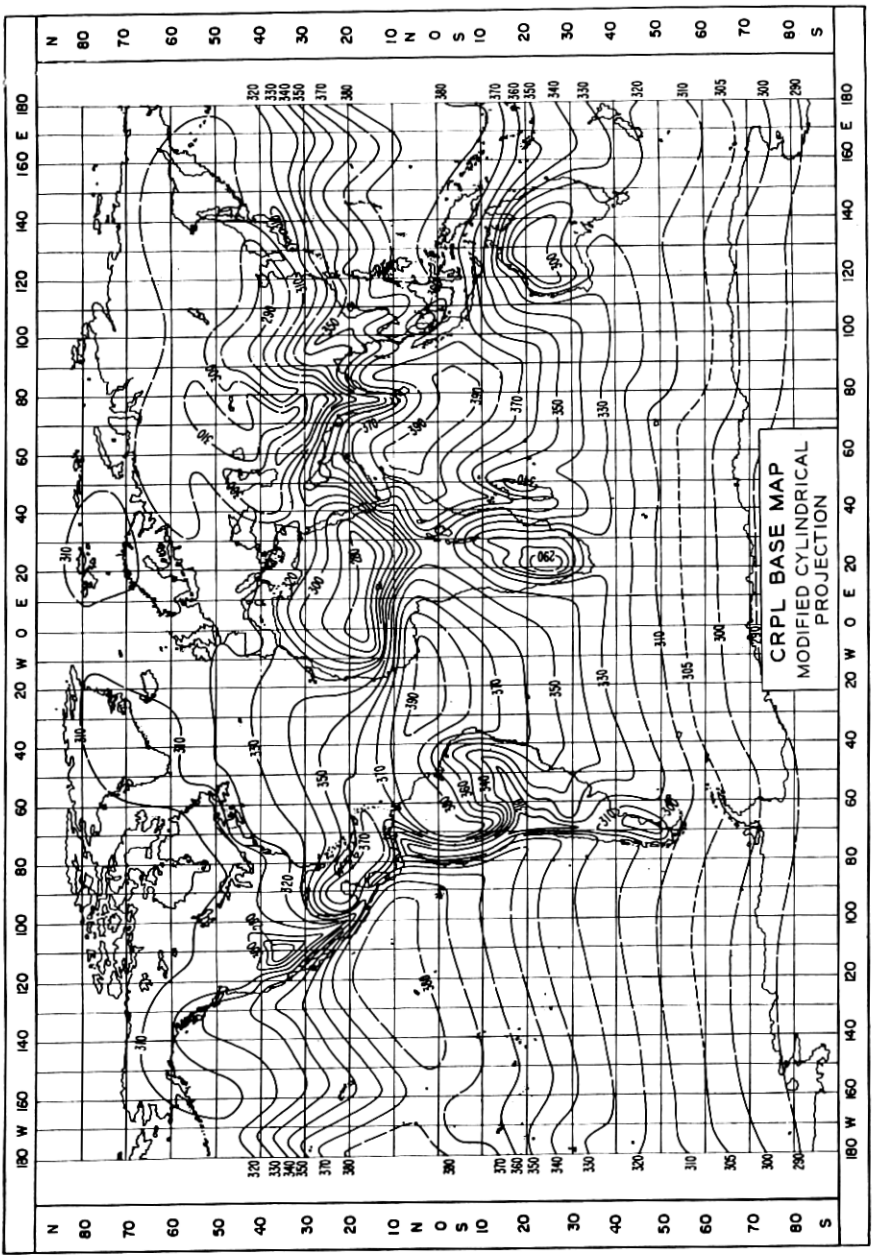

Fig. 2—Minimum monthly mean value of N (Taken from Ref. 6).

determined for the specific path under study. We need, then, to determine the relation between K and refractivity.

A method for determining the approximate value of K for a given path is developed in Appendix A. The initial step in the procedure requires the selection of appropriate values of minimum monthly mean refractivity at sea level, N_o, for the geographical coordinates of the stations at each end of the path. Fig. 2 gives such data, collected from 306 weather stations over a period of years.

Next, values of refractivity, N_s, are calculated for the altitude at each station. This is done using equation (22), repeated here for convenience as:

$$N_s = N_o \exp(-0.0322h) \tag{3}$$

where N_o and N_s are in "N-units," and h is the station altitude, in thousands of feet.

Finally, the values of K corresponding to the surface refractivity at each station are read from Fig. 3, and a single average for the path is estimated from the values at the end points. Unless the path is very long

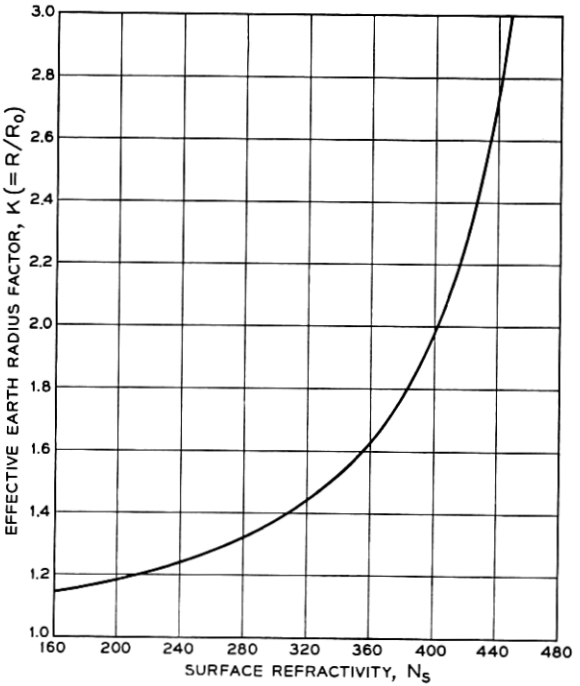

Fig. 3 — Effective earth-radius factor vs refractivity at surface.

or there is a large difference between the altitudes of the two stations, the values of K determined for the two stations are likely to be almost the same.

2.3 *Effect of a Difference in Antenna Site Altitude*

The angle θ for a symmetrical path with no obstructions can be determined by consideration of refractivity alone, as outlined above. When the altitudes of the antenna sites above sea level are significantly different, or when the antenna centerlines are directed above or below the horizontal, corrections are necessary to determine the angles of the beam centerlines above the chord. The correction factors may be (and generally will be) different at the two ends of the path. The effect of a difference in altitude of antenna sites will be considered first.

Fig. 4(a) illustrates the geometry of an unsymmetrical path. The asymmetry here is due to the high altitude above sea level of the antenna at the left. For paths of practical interest, the difference in altitude, Δ, between antenna sites is not likely to exceed a few thousand feet. (The

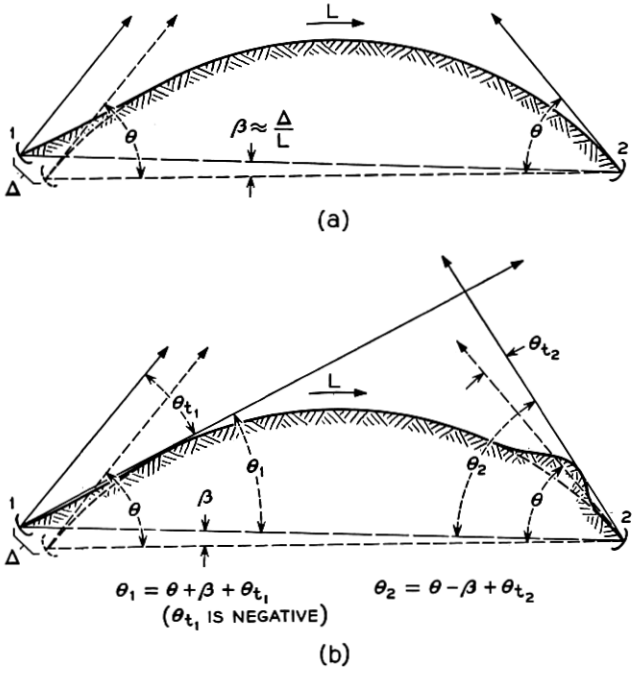

Fig. 4 — (a) Antenna 1 at altitude Δ above Antenna 2; (b) negative take-off angle at raised site 1, positive take-off angle at site 2.

greatest difference in existing systems known to the authors is about 8000 feet, on a path in the Arctic.) Thus, since Δ is very small relative to the path length, L, the correction angle β to account for the elevation difference is given with sufficient accuracy by

$$\beta \approx \frac{\Delta}{L} \tag{4}$$

2.4 *Effect of Nonhorizontal Antenna Take-Off Angle*

When an antenna site is elevated and there is no foreground obstruction the beam centerline axis is generally depressed from the horizontal and aimed at the optical horizon to increase the received signal. Conversely, when there is an obstruction between an antenna and the normal horizon it may be necessary to elevate the antenna axis above the horizontal.

In the case of Fig. 4(a), for example, the beam from the elevated antenna at the left would normally be depressed by an angle θ_{t1} in aiming at the horizon. This is illustrated in Fig. 4(b). Also in Fig. 4(b), an obstruction has been added in front of the antenna at the right, requiring that its beam axis be elevated by angle θ_{t2} . θ_t at either end will be considered positive when measured upward from the horizontal.

By combining the effects of antenna altitude difference and nonhorizontal take-off angles, the following general expressions are obtained for the angles θ_1 and θ_2 between the chord joining the antenna sites and the centerlines of the respective antenna beams:

$$\theta_1 = \theta + \beta + \theta_{t1} \tag{5}$$

$$\theta_2 = \theta - \beta + \theta_{t2} \tag{6}$$

where θ is defined by (2), β is defined by (4), and θ_1 is at the end with greater altitude. The factor β generally can be ignored if the antenna sites are within about a thousand feet of the same altitude above sea level.

2.5 *Concept of "Echoes"*

The conventional diagram for a tropospheric scatter path, as illustrated in Fig. 1, shows well-defined antenna beams projecting from each terminal. This is a convenient model for many purposes, particularly for determining received signal power. It can be misleading when one is concerned about interference effects, however. We will therefore discard the notion of a bounded antenna beam, and turn instead to the geometry illustrated in Fig. 5.

In this illustration, the earliest-received — and generally the strongest

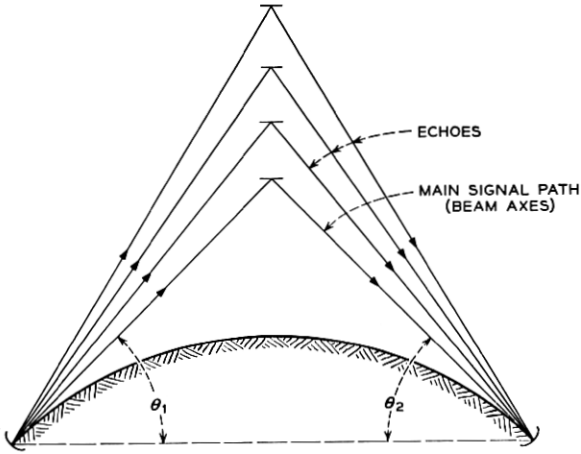

Fig. 5 — Illustration of tropospheric transmission in terms of "main signal" and "echo" paths.

— signal component travels along the axes of the antenna beams and is reflected at their intersection in the troposphere. This will be called the "main signal." Other components of signal are assumed to be smaller in amplitude because they are somewhat off the maximum-gain centerline of the antenna beam, and also because the reflected power decreases with increasing altitude of the reflection point. These reflections will be called "echoes" because of their delay behind the main signal.

Although there must be an infinitely large number of echoes from a continuously illuminated common volume, some sections of the volume probably produce higher power density than others as seen by the receiving antenna. It is helpful in this argument to consider the total received power as some equivalent result of a finite number of signal paths.

In the remaining analytical sections of this paper, it is assumed that reflections occur independently, at random, and only in the plane of the antenna beam centerlines. Among the entire ensemble of such echoes, one is to be designated as the "worst" echo — the echo calculated to produce most distortion in the output of the system. Other echoes — including those on either side of the beam centerlines — will contribute to the total distortion, but their effects are included later as part of the empirical correction for multiple echoes.

2.6 *Summary of Model*

The results up to this point can be summarized as follows: A path structure has been proposed which replaces the conventional 3-db an-

tenna beamwidth by a series of signal paths. The shortest of these paths is assumed to follow the antenna beam centerlines, and is designated the main signal path; the rest are echo paths. Critical parameters in the model are the angles θ_1 and θ_2 between the antenna beam centerlines and the chord joining the two antenna sites. The received power, given by (1), depends critically on these angles. When the path geometry is symmetrical, (which would be the case with both antennas at sea level and no foreground obstructions), the angles depend only on path length and atmospheric refractivity (2). When there is a significant difference in the altitudes of the antenna sites or non-horizontal antenna take-off angles, θ_1 and θ_2 must be modified accordingly (5, 6).

The foregoing model will be used in deriving expressions for echo amplitude, echo delay, and finally, intermodulation.

III. ECHO AMPLITUDE

The magnitude of an echo relative to the main signal over a tropospheric scatter path is derived in Appendix B. The derivation makes use of (1) to express the power received in vanishingly small beamwidths α and α_e, representing main signal and echo paths at angles θ and θ_e, respectively (See Fig. 6). The "reflection loss," r_e, of the received echo power relative to the received main signal power is given by (28); thus:

$$r_e \text{ (in db)} = 10 \log_{10} \left(\frac{\theta_e}{\theta}\right)^7 = 10 \log_{10} \rho^7. \tag{7}$$

It can be shown that (7) is valid for the unsymmetrical path of Fig. 7

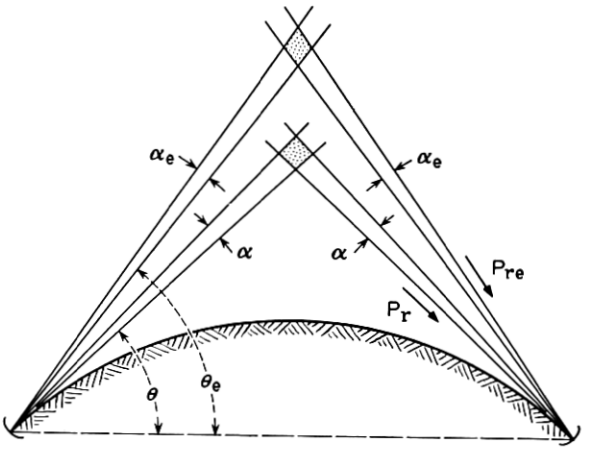

Fig. 6 — Geometry used to calculate ratio of main signal power to echo power in a symmetrical path (7).

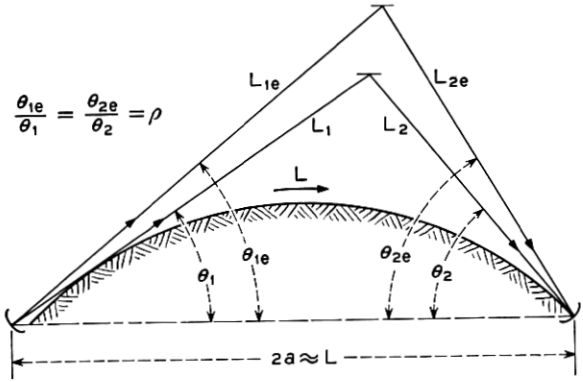

Fig. 7 — General unsymmetrical path.

as well, where the main signal and echo angles are related by:

$$\frac{\theta_{2e}}{\theta_2} = \frac{\theta_{1e}}{\theta_1} = \rho \tag{8}$$

Equation (7) also holds for the "small layer" version of the reflection theory. For the "large layer" theory, which may be more applicable under high-signal conditions, the reflection loss r_e can be shown to vary as $(\rho)^9$.

The derivation of (7) assumed that the antenna gains in the directions of the echo path were equal to the gains along the main signal path. In many cases, particularly those involving half-power beamwidths less than about one degree, the difference in antenna gain between the angles of the echo and main signal paths will add a significant factor to the difference between the received echo and main signal powers. Thus, if the combined loss due to the decrease in the radiation patterns of the two antennas at the angles θ_{1e} and θ_{2e} is given by r_a, in db, the resultant ratio of main signal to echo power is:

$$r \text{ (in db)} = r_e + r_a . \tag{9}$$

The reflection loss, r_e, is related to ρ by (7). The antenna loss, r_a, can be determined with sufficient accuracy from antenna patterns such as those illustrated in Fig. 8. The beam axes correspond to angles θ_1 and θ_2. Thus, the antenna losses at the echo angles θ_{1e} and θ_{2e} can be read from the appropriate antenna patterns at angles from the axes given by

$$\theta_{1e} - \theta_1 = (\rho - 1)\theta_1 \tag{10}$$

at one end of the path and

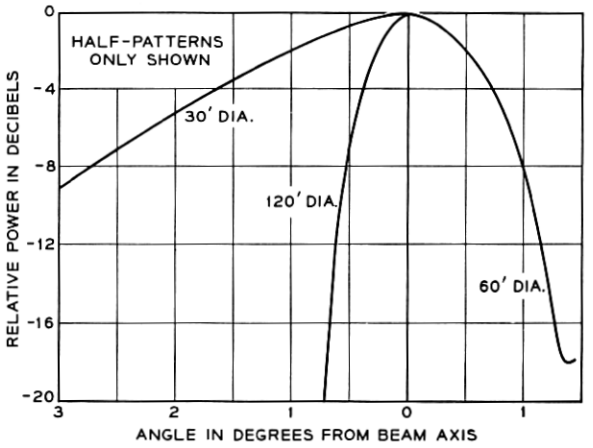

Fig. 8 — Typical free-space patterns of parabolic antennas (750 mc).

$$\theta_{2e} - \theta_2 = (\rho - 1)\theta_2 \tag{11}$$

at the other.

IV. ECHO TIME DELAY

The time delay of an echo traveling the path θ_{1e}, θ_{2e} relative to the main signal traveling the path θ_1, θ_2 (Fig. 7) is:

$$T = 2.68\ L\ \theta_1\theta_2(\rho^2 - 1) \text{ microseconds.} \tag{12}$$

Here the path length, L, is in statute miles and ρ is as defined by (8). The derivation of (12) is given in Appendix C.

V. INTERMODULATION, SINGLE ECHO

A method for calculating intermodulation distortion caused by a single echo in the transmission medium of an angle-modulated system is given in Ref. 4. The method assumes a baseband loaded with random noise simulating many frequency-division multiplexed voice channels. The signal-to-intermodulation ratio, S/I, in a narrow frequency slot anywhere in the baseband output can be computed for given values of signal-to-echo power ratio (r), echo delay (T), base bandwidth (f_b)* and rms frequency deviation (σ). The technique is applicable for signal-to-echo power ratios greater than about 5 or 6 db.

* The theory presented in Ref. 4 assumes that the baseband extends from zero to a top frequency f_b. In practical systems, the lower edge of the band starts at some nonzero frequency, say 12 kc. For systems of many channels, the assumption of a band extending to zero introduces negligible error.

Figure 5.7 in Ref. 4 shows a set of curves from which one can determine the S/I ratio in the top channel of an FM system without pre-emphasis. Fig. 9 is a similar set of curves computed for a pre-emphasized FM system. The preemphasis characteristic, Fig. 10, is typical of those used on many tropospheric scatter systems. The curves of Fig. 9 are probably also sufficiently accurate for phase modulation.

Fig. 9 is used as follows:

Given values of base bandwidth, frequency deviation, and an assumed value of time delay, compute the rms deviation ratio, σ/f_b, and the product of top baseband frequency and echo delay, f_bT. Note the value of the contour line on Fig. 9 at the intersection of the lines for the computed values of σ/f_b and f_bT. The value of the contour at the intersection

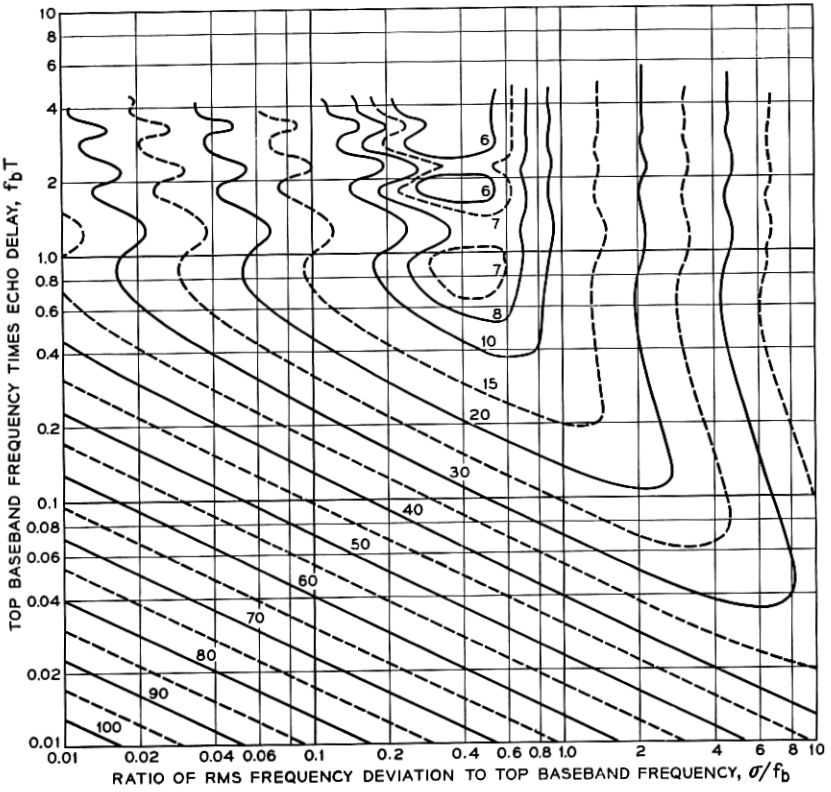

Fig. 9 — Contours of constant interference. (Value in db by which S/I ratio exceeds signal-to-echo power ratio in multichannel pre-emphasized FM system. Value is for top channel only.)

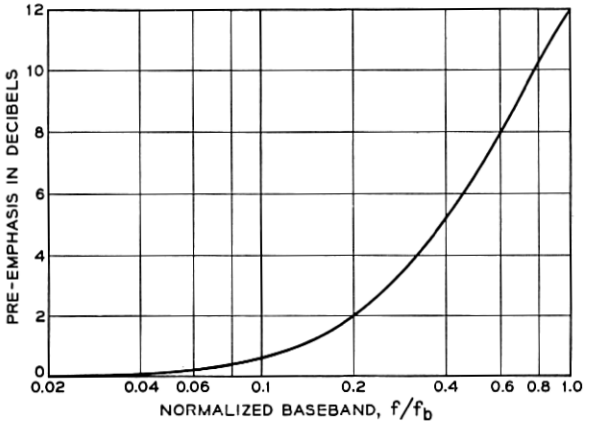

Fig. 10 — Pre-emphasis typical of tropospheric scatter systems.

represents the amount by which the S/I ratio *exceeds* the received signal-to-echo power ratio, r, in db. Thus, the values of the contour and the signal-to-echo power ratio must be added to arrive at the S/I caused by the echo.

The manner in which S/I varies as a function of echo time delay can be determined from Fig. 9, for a system of given parameters and a single echo of known magnitude. A family of curves of S/I vs. time delay can be developed, where each curve in the family applies to an echo of fixed amplitude. Fig. 11 shows such a family. The particular case chosen for illustration is that of a one-megacycle baseband, pre-emphasized and frequency modulated with an rms deviation ratio of one. Each line of this family of curves corresponds to a cross-section of the contours of Fig. 9 on the vertical line $\sigma/f_b = 1.0$. To the cross-section from Fig. 9 has been added, in the case of each curve on Fig. 11, the indicated signal-to-echo power ratio r.

Note that the family of curves in Fig. 11 applies generally to any system having the selected base bandwidth and deviation. It has not been tied to any particular path. The problem now is to find the combination of echo amplitude and delay time for a selected path which produces the most distortion in the system. To illustrate the method of doing this, the following path parameters have been arbitrarily chosen:

Path length, $L = 200$ miles

Refractivity factor, $K = \frac{4}{3}$

Antennas, both ends = 60-foot parabolas, with patterns as in Fig. 8

A symmetrical path

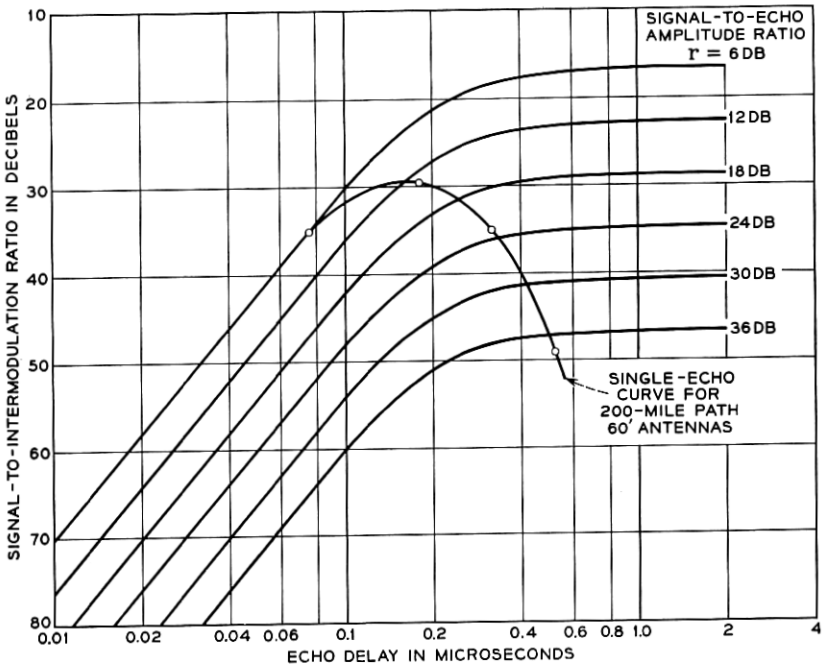

Fig. 11 — S/I vs echo delay (single echo) for pre-emphasized FM; f_b = 1.0 mc, σ/f_b = 1.0.

Equation (2) is used to calculate $\theta_1 = \theta_2 = 0.019$ radians. This is the angle between the chord separating stations 200 miles apart, and the antenna beam axis for a horizontal take-off angle.

Next, choose an arbitrary value of reflection loss, r_e. Suppose 5 db is chosen, corresponding to the power ratio 3.16. This is the ratio of the *reflection* loss along some echo path at angle θ_e, to the reflection loss along the main signal path at angle θ_1 (or θ_2). To this value of reflection loss must be added the reduction in antenna gain at the angle of the echo.

To find the reduction in antenna gain at the angle θ_e corresponding to 5 db reflection loss, first compute ρ from (7). Then (10) or (11) can be used to compute the angular difference $(\theta_e - \theta_1)$ or $(\theta_e - \theta_2)$. The difference in this example turns out to be 0.19°. At this angle from the beam axis of a 60-foot antenna, Fig. 8 shows that the antenna loss, r_a, for *two* antennas at the angle of the echo path is about one db. The total loss

along the echo path, relative to the main signal path, is then r_e (5 db) plus r_a (1 db), or 6 db.

The time delay of this echo, given by (12), is about 0.075 microseconds.

Turning now to Fig. 11, the S/I ratio corresponding to the echo delay $T = 0.075$ microseconds and the echo amplitude ratio $r = 6$ db is about 35 db.

Similar computations are now performed for other arbitrarily-selected values of reflection loss, say 10, 15, and 20 db. Each case is associated with a separate echo path, and the total echo loss and delay along that path is computed. The results of such calculations are summarized in Table I, together with the S/I ratios that each echo individually would

TABLE I — EXAMPLE OF SINGLE-ECHO S/I CALCULATION

Reflection Loss, r_e (db)	Two-Ant. Loss, r_a (db)	Total Loss, r (db)	Delay T (μsec)	$\frac{S/I}{(\text{db})}$
5	1	6	0.075	35
10	3	13	0.18	30
15	8	23	0.32	35
20	18	38	0.52	50

produce if it were the only contributor. These values of S/I are also plotted on Fig. 11, resulting in the overlay curve showing how S/I varies with echo delay and amplitude for the specific path used in the example.

The important point to note in Fig. 11 is that there is a peak in the S/I intersection curve, occurring at time delays near 0.16 microsecond for the 200 mile example path and the assumed baseband and deviation. This tendency toward a "worst echo" effect has been found to be characteristic of all paths studied. The location of the peak on the time delay scale varies depending on the path length, base bandwidth, deviation, and other parameters involved. In particular, it has been observed that, as path length increases, the peak of the intersection curve for wide frequency deviations tends to shift to the region of echo amplitude r less than 5 or 6 db. It is in this region that the intermodulation theory loses accuracy. This has not appeared to be a serious limitation in work to date, however.

VI. LIMITATIONS OF THE ANALYTICAL METHOD

The analytical method as outlined predicts the intermodulation in the output of a receiver due to a single echo, when the received power is assumed given by (1). There are three significant limitations to the method at this point:

(*i*) It predicts a single fixed value of intermodulation, whereas measurements show that there are both long-term changes in the average value as well as more rapid variations about an average during a short interval.

(*ii*) The analysis predicts the effects of single echoes only; practically, there must be a continuum of echoes spread over something vaguely defined as a "common volume," and the total intermodulation generated by these echoes is bound to be greater than that of a single "worst" echo.

(*iii*) The theory of intermodulation due to transmission echoes as presented in Ref. 4 is valid only for echo amplitudes smaller than about 5 or 6 db relative to the main signal. On tropospheric paths, theory suggests that the strongest echoes are normally associated with the shortest time delays. Having short time delays, they would not contribute greatly to interchannel modulation, although they would be responsible for signal fading and the associated increases in fluctuation noise during fades. This is not the entire story, however. While strong echoes may *normally* be associated with short time delays, there are surely some meteorological conditions which produce strong reflecting or scattering regions at abnormally high altitudes. Occasionally, then, an echo might be comparable in magnitude to the main signal *and* be delayed enough to cause severe distortion. It should be emphasized that this apparently is not the average situation, which is of primary concern in this paper.

Efforts to develop satisfactory analytical techniques to remove the limitations noted above have thus far been unsuccessful. Empirical corrections have therefore been developed to account for them, based on the comparison of calculated values and results of tests presented in the following section.

VII. COMPARISON OF CALCULATED AND MEASURED INTERMODULATION

Measurements of intermodulation have been made on four tropospheric scatter paths with diverse climates, path lengths, and siting conditions. Significant parameters of the four paths are given in Table II.

The four systems were Gaussian-noise loaded except for a slot near the top of the baseband. Median values of interference power were measured in this slot at the receiver during approximately $1\frac{1}{2}$ to 3-minute samples. The median of each sample was adjusted to account for fluctuation noise and equipment intermodulation, leaving the value of intermodulation noise chargeable to the path. A more detailed account of test procedures and methods of data analysis is given in Ref. 7.

Table III shows a comparison of the raw measured non-diversity

TABLE II — PARAMETERS OF FOUR TEST PATHS

	Path 1		Path 2		Path 3		Path 4	
	Trans.	Rec.	Trans.	Rec.	Trans.	Rec.	Trans.	Rec.
Location	Caribbean (over water)		Arctic (over ice)		Arctic (over water)		Arctic (over water)	
Length, Statute Miles	185		194		440		340	
Radio Freq., mc (Nominal)	725		900		900		800	
Ant. Dia., ft.	60	60	30	60	120	120	120	120
Site Elev., ft. (Above Sea Level)	200	10	8000	1100	70	1100	700	1100
Eff. Earth Radius Factor, K	1.55		1.26		1.37		1.38	
Ant. Takeoff $\measuredangle$, θ_t, radians	0	≈ 0	-0.0035	-0.004	-0.010	-0.0026	-0.0005	-0.0014
$\measuredangle$'s Between Ant. Axes and Chord, θ_1 and θ_2, Radians	0.0151	0.0151	0.0227	0.0087	0.0375	0.0309	0.0295	0.0308

results from the four test paths and the results calculated for the single "worst" echo. The same data are presented as a scatter plot in Fig. 12. With the exception of the Path 2 data, each point represents an average of the median values from at least 5 to as many as 20 test samples, for one combination of base bandwidth and frequency deviation. Only 3 samples were available for each combination from the Path 2 tests.

VIII. ADJUSTMENT OF MEASURED INTERMODULATION TO WORST-MONTH PROPAGATION CONDITIONS

Results from the four tropospheric scatter test paths have shown that there is a decided correlation between average intermodulation and average path loss (or received power). As path loss increases, intermodu-

TABLE III — COMPARISON OF SINGLE-ECHO CALCULATIONS AND RAW MEASURED S/I, DB

Top Baseband Freq., kc	RMS Dev., kc*	Path 1		Path 2		Path 3		Path 4	
		Calc.	Meas.	Calc.	Meas.	Calc.	Meas.	Calc.	Meas.
108	62	—	—	—	—	51	38	—	—
	125	—	—	68	48	45	35	51	47
	250	—	—	62	43	40	31	45	43
	500	—	—	57	37	36	30	41	38
	800	—	—	54	33	36	32	—	—
	1000	—	—	—	—	—	—	40	33
300	62	—	—	—	—	43	32	—	—
	125	—	—	59	43	37	28	42	41
	250	55	48	53	38	32	27	37	37
	500	49	41	48	33	27	27	32	32
	800	—	—	45	30	26	27	—	—
	1000	45	36	—	—	—	—	30	28
	2000	43	34	—	—	—	—	—	—
552	62	—	—	—	—	37	31	—	—
	125	—	—	53	36	31	27	37	35
	250	50	42	48	33	26	24	32	32
	500	44	36	43	29	22	24	27	27
	800	—	—	40	27	21	23	—	—
	1000	40	29	—	—	—	—	25	23
	2000	37	28	—	—	—	—	—	—
1052	125	—	—	49	30	—	—	—	—
	250	44	37	43	27	—	—	33	27
	500	39	32	37	23	—	—	27	25
	800	—	—	34	21	—	—	22	22
	1000	35	26	—	—	—	—	—	—
	2000	32	24	—	—	—	—	20	18

* The deviations used on Path 3 were slightly smaller than listed here. In each case, however, calculated values of S/I are given for the actual deviations used in tests.

lation also increases. While the relationship between path loss and intermodulation may not be highly obvious from the various equations presented to this point, the fact that intermodulation does vary and that a correlation with path loss shows up in measured data leads to the following questions:

(*i*) To what value of path loss does the computed value of intermodulation correspond? In other words, what is a useful point of reference for the observed dependence?

(*ii*) What is the rate of variation of intermodulation with path loss?

The point of reference for the relation between intermodulation and path loss has already been suggested in the earlier discussion of refractivity. It was indicated there that in calculating the effective earth radius

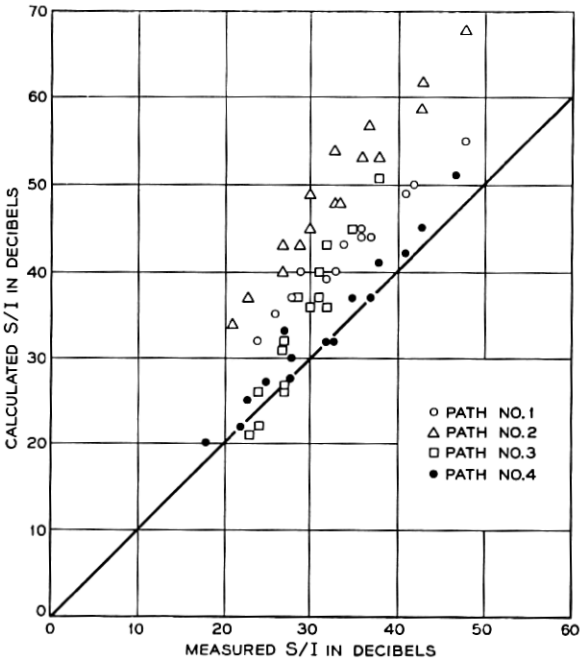

Fig. 12 — Calculated single-echo S/I vs average measured (unadjusted) S/I.

factor, K, the minimum monthly mean value of refractivity indicated in Fig. 2 should be used. Minimum refractivity corresponds to minimum bending of the radio waves, maximum values of antenna centerline angles θ_1 and θ_2, maximum time delay for an echo of given amplitude, and therefore maximum intermodulation. Correspondingly, (1) indicates that minimum refractivity (maximum θ) tends to minimize the average received power. Thus, the observed direction of variation of intermodulation and path loss is borne out by our model. It may be deduced that the value of intermodulation computed on the basis of minimum monthly mean refractivity corresponds directly to what is commonly called "worst-month" path loss — the monthly median path loss during the worst, month-long period of propagation during the year. (There should be some probability attached to this value, but it is usually approximated without this refinement.) Estimates of worst-month loss on a new path are generally derived from data from other paths, with subsequent adjustment based on measurements over the new path.

It can be noted that the choice of worst-month conditions as the point of reference is somewhat arbitrary. We might have chosen instead to use

an average annual value of refractivity, compute an average annual value of intermodulation, and relate the latter to the average annual path loss.

Apart from the point of reference chosen, there remains the second question posed above: what is the rate of variation of intermodulation with path loss, for propagation conditions other than the reference condition? If data were available on the time variations of refractivity for any path of interest, it might be possible to compute an approximate relationship. Unfortunately, such detailed refractivity data are not generally available. As a substitute, we are forced to use empirical adjustments based on results of measurements of intermodulation and received power.

Fig. 13 is typical of the data which have been obtained. Shown are two plots of intermodulation (in terms of S/I ratio) versus received signal measured on Path 3 — a 440-mile over-water path in the Arctic. Each point represents the median values of the two variables during a test sample of about 90 seconds. The total test period covered about ten days, during which time a wide range of propagation conditions was encountered. The rather wide scatter of points is an indication that factors other than *average* path loss can affect the value of intermodulation during any specific test sample. For example, a localized region of high reflecting ability could produce a strong echo and unusually high intermodulation.

The data of Fig. 13 apply for a base bandwidth of 300 kc, rms frequency deviations of 125 and 250 kc, and no receiver diversity. The slope of the curve drawn through the 125 kc deviation scatter plot is slightly greater than one; that is, intermodulation and path loss varied

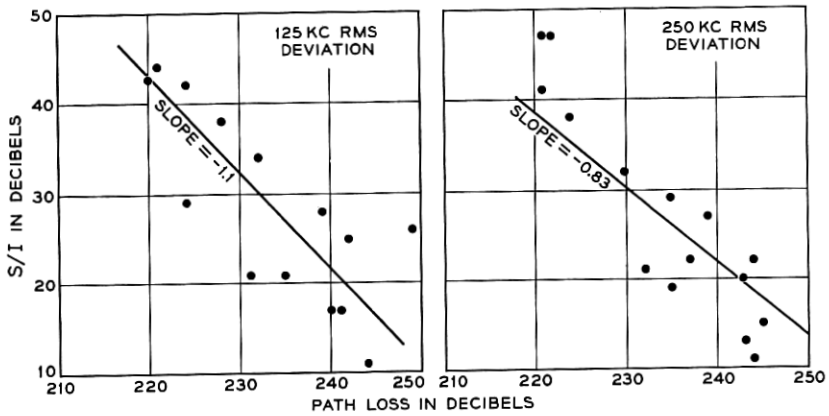

Fig. 13 — S/I vs path loss — 440-mi arctic path, 300-kc baseband, no diversity.

approximately db for db. The slope of the 250 kc plot is slightly more than 0.8. The least squares method was used to calculate these slopes.

Similar scatter diagrams plotted for other combinations of these transmission parameters and the other three paths indicate that the change in intermodulation ranged from about 0.4 db to 1.2 db per db of path loss change. The lowest values were noted on Path 1 — a 185-mile path between Florida and Cuba. There was no apparent pattern to the slopes of the scatter plots as a function of baseband or deviation on any of the four paths tested, except that the slope was generally lowest for the highest deviation ratio. There is a technical justification for the latter effect contained in the contour curves of Fig. 9. Note that a variation in time delay of an echo of given amplitude represents a change in the ordinate f_bT on these curves. It is clear that for a given change of time delay (say, corresponding to a change in f_bT from 0.1 to 0.2), a system operating at a high deviation ratio (toward the right on the σ/f_b scale) will in general exhibit a smaller change in S/I than will a system operating at a low deviation ratio. Except for this trend, however, the effects of different path lengths, antenna sizes, take-off angles and climates confound any attempt to find a precise dependence of S/I on path loss.

The data referred to above, together with similar data from three other paths, indicate that an adjustment to the computed value of S/I of about 0.7 db per db of path loss change is reasonable when one is trying to predict the probable average value of S/I for a path at times other than the worst month. If one is trying to compare a computed worst-month value of S/I with results of measurements on a specific path, it will be more accurate to determine the average slope of scatter plots similar to those of Fig. 13, and use that slope to place the computed and measured results on a comparable path loss basis. Thus, the correction to be added to the median measured S/I during a test period to adjust it to worst-month conditions can be expressed as:

$$D = S(TPL - WPL) \tag{13}$$

where S is the average slope, TPL is median path loss during the test period, and WPL is the worst-month median path loss.

During the test periods for which the results in Table III and Fig. 12 apply, the median path losses on Paths 1, 3 and 4 were four to eight db less than worst-month estimates. During the tests on Path 2, which were conducted over a period of 10 days, the median path loss was about 8 db greater than the worst-month median estimate. Thus, adjustments to the measured data are necessary to convert them to propagation conditions comparable to those assumed in calculations. This was done as follows:

For each path, the average slope was determined of the least-squares lines drawn through scatter plots of S/I versus path loss (similar to those illustrated in Fig. 13). The average slope was then used to adjust the measured S/I results to the worst-month path loss condition, using (13). The estimated worst-month median path losses, test period median path losses, and the slopes used for the S/I adjustments for each of the four test paths are given in Table IV.

TABLE IV

	Path 1	Path 2	Path 3	Path 4
Worst Month Median Path Loss (WPL)	197 db	213 db	243 db	240 db
Test Period Median Path Loss (TPL)	193 db	221 db	235 db	236 db
Avg. Slope of S/I vs Path Loss	0.5	0.7	0.9	0.6
Total Adjustment to Measured S/I Data	−2 db	+6 db	−7 db	−2 db

When the adjustments indicated in the last line of Table IV are made to the measured data plotted in Fig. 12, the result is as given in Fig. 14. With the exception of the Path 3 data, the adjusted points exhibit a noticeably narrower spread than before the path loss adjustments were made. However, the group of points as a whole still differs significantly from the calculated results for single echoes.

IX. ADJUSTMENT OF CALCULATED INTERMODULATION TO ACCOUNT FOR MULTIPLE ECHOES

It has been emphasized that a calculated value of intermodulation represents only the contribution of the single worst echo among echoes which have at least 5 or 6 db lower amplitude than the first-arriving signal element. In fact, however, there are probably very many echoes present at any given time on a tropospheric scatter path. The combined effects of a multiplicity of echoes is to produce more intermodulation than the maximum attributed to any single echo. Thus, it seems qualitatively reasonable to attribute the remaining differences between calculated and measured results in Fig. 14 to the effects of multiple echoes.

The results for Paths 1 and 2 in Fig. 14 appear to be closely intermingled, and they differ from the calculated values for single echoes by an average of about 10 db. The Path 4 results form a group somewhat closer to calculated values; their average difference is only about 4 db. As already noted, the differences for Path 3 vary more widely. This is thought

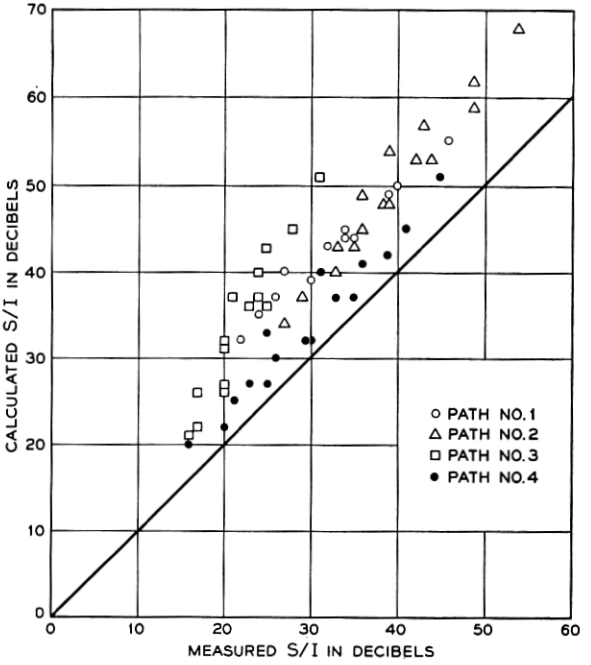

Fig. 14 — Calculated single-echo S/I vs average measured S/I normalized to worst-month path loss conditions.

to be at least partially the result of a propagation anomaly observed on this path, the effects of which will be discussed shortly. There are also a number of other recognized sources of possible errors in both the calculated and measured data, and these will also be discussed. Since there is no way at this time to resolve the quantitative effects of these errors, we are left with the undesirable but rather inescapable alternative of trying to estimate an adjustment for multiple echoes from the scatter of points as they stand in Fig. 14.

Fig. 15 shows the result of subtracting nine db from each point in Fig. 14. This value gives a little extra weight to the data from Paths 1, 2, and 3 for the following reasons: (a) there is relatively good agreement among the adjusted data for these three paths, and (b) up to the time of this writing, there has been considerable uncertainty as to the path loss data which should be assumed for Path 4.

While 9 db appears to be a reasonable average adjustment, it should not be expected that the intermodulation measured during any single test sample would be 9 db more than the calculated figure. The number

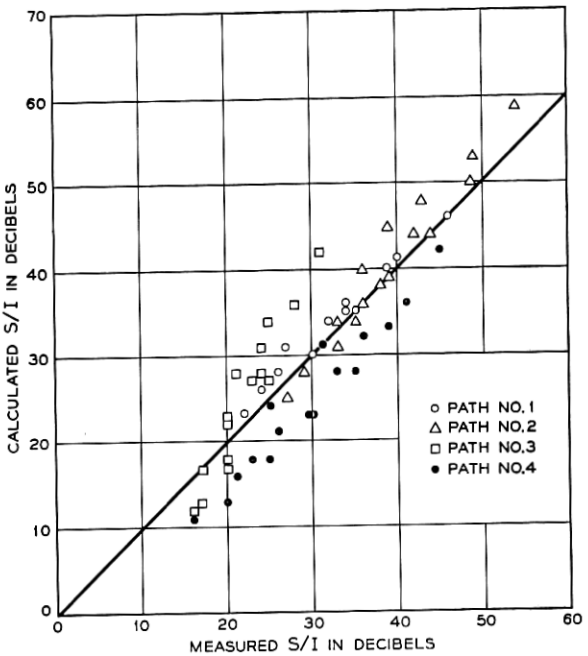

Fig. 15 — Calculated S/I adjusted for multiple echoes vs average measured S/I normalized to worst-month propagation.

of significant echoes is bound to vary from test sample to test sample as atmospheric conditions change. We are aware, too, of various sources of error in calculated or measured results. These errors are discussed in a later section, and it will be apparent that some of them can have an effect on the values assumed for path loss and multiple echo adjustments.

With the caution that some change in the number can be expected as better understanding and more and better data become available, it is felt that nine db is a reasonable number to account for the effects of multiple echoes in calculations of path intermodulation.

X. ANOMALY ON PATH 3

Fig. 15 shows that there is a wider variation of differences between measured and calculated results for Path 3 than for the other paths. This might be explained by the fact that the extreme length of the path makes it possible for strong reflections from the tropopause to cause more interference, at times, than echoes in the troposphere alone. The altitude of the tropopause over Path 3 was reported at 25,000 to 35,000 feet from

day to day during the test period. When the tropopause is in the lower half of this range, according to the method of calculation described earlier in this paper, reflections could cause distortion that is significant with respect to the maximum from a single echo in the troposphere. The effect is greatest for low FM deviations, as indicated by the calculated results in Table V.

Fig. 16 shows the same comparison as Fig. 15 except that on Path 3, a reflection is assumed to occur at 27,000 feet with no more reflection loss than the main signal. Thus, the echo at the receiver would be reduced below the main signal only by the antenna losses due to the elevated angles of the path to the tropopause. In plotting Fig. 16, the interference from this echo was added to the single echo maximum before making the 9 db correction for multiple echoes.

To make the calculated S/I for Path 3 correspond even better with the measured values, it would be necessary to weigh the effect of reflections from the tropopause more heavily than the effects of the tropospheric reflections. One way to increase the effect of the tropopause reflections would be to assume its altitude to be 25,000 or 26,000 feet. Another possibility is to assume that the tropopause provides a better reflecting surface than do the layers in the troposphere, so that, except for the antenna loss, the echo from the tropopause would be stronger than the main signal.

Still another possibility is contained in the following argument. In

TABLE V — EFFECT OF TROPOPAUSE ON S/I RATIOS, PATH 3

Top Baseband Frequency, kc	RMS Dev., kc	Calculated S/I, db				Measured S/I	
		Tropo-sphere Single Echo	Tropo-pause Echo, 27,000′	Sum of First Two Echoes	9-db Corr., Multiple Echoes	Raw	Adj. to Worst Month
108	62	51	49	47	38	38	31
	125	45	44	41	32	35	28
	250	40	41	37	28	31	24
	500	36	44	35	26	30	23
	700	36	50	36	27	32	25
300	62	43	42	39	30	32	25
	125	37	36	33	24	28	21
	250	32	33	29	20	27	20
	500	27	36	27	18	27	20
	800	26	41	26	17	27	20
552	62	37	38	34	25	31	24
	125	31	33	29	20	27	20
	250	26	29	24	15	24	17
	500	22	31	22	13	24	17
	800	21	36	21	12	23	16

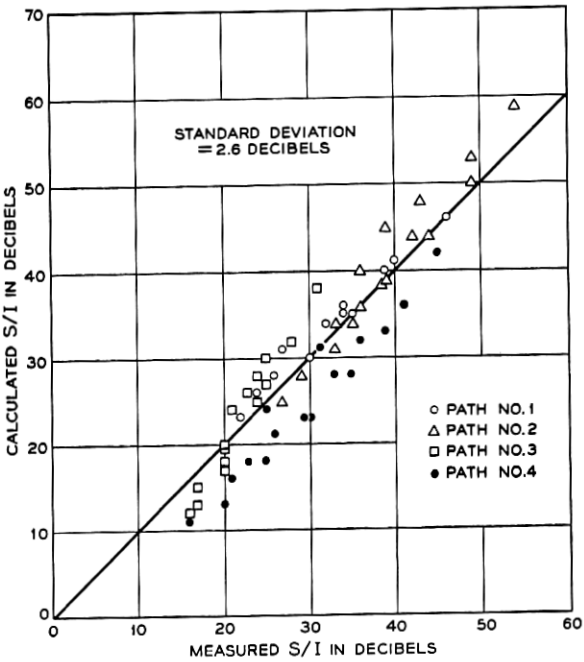

Fig. 16 — Calculated vs measured S/I when tropopause reflection is added to calculated results for path 3.

applying the model of the tropospheric scatter path described in this article, the power in the lower half of the antenna beams has been neglected as though it were blocked by the horizon. Suppose that power in the lower half of the antenna beam grazing the surface of the sea were reflected (and spread somewhat by the convexity of the surface) with negligible loss. This power, with almost no antenna loss, may be reflected again from the tropopause and cause high distortion because of its long delay and low loss. This argument is particularly suited to Path 3 where the antennas at one end are located on a cliff 1100 feet above the sea.

There seems little point in speculating further about the reasons for the relatively peculiar behavior of the results for this path. While each of the arguments above has some plausibility, the fact remains that information is not now available to prove any of them.

XI. SOURCES OF ERRORS IN CALCULATED AND MEASURED DATA

The foregoing comparison of calculated and measured results indicates that the analytical-empirical method of predicting intermodulation has a standard error of estimate of about 2.6 db relative to measured results.

Part of this error is due to the limited accuracy of the empirical adjustments for path loss and multiple echoes. There are in addition a number of other possible sources of error in both the calculated and measured data, and these will now be discussed.

11.1 *Path Loss Data*

Estimates of worst-month path loss are difficult to make, and errors of 2 or 3 db are not unlikely. In fact, different methods of estimating path loss show that much discrepancy.

Determination of the median path loss from tests is also subject to errors. Knowledge of the values of transmitter output power, received signal power, RF plumbing losses, and antenna gains is required, and inevitably some error creeps into measurements of these parameters. Any error in such measurements should be approximately constant (assuming negligible changes between test periods) for a given path. Hence, it should not affect the slope of an S/I versus path loss scatter plot for that path. However, a constant error would affect the value of the adjustment used for multiple echoes.

11.2 *Antenna Orientation and Pattern*

Ideal free-space antenna patterns and centerlines directed at the horizon are assumed in calculating intermodulation by the method outlined in this paper. In practice, local siting conditions may have some effect on an antenna pattern and modify the assumed amplitude relationship between echoes at different angles from the horizon. The errors due to these factors should be a constant for any one path, but when the results for several paths are brought together as in Figs. 13 to 16, they will contribute to the spread of data.

The antenna patterns assumed in all the calculated results in this paper were those shown in Fig. 8. These patterns — determined from scale-model measurements — apply at a frequency of about 750 mc. As Table II indicates, the frequencies on the test paths varied from about 725 mc to 900 mc. In view of the uncertainty noted above relative to effects of local siting conditions, it has not appeared worthwhile to adjust the nominal patterns for 750 mc to patterns for specific test frequencies; however, it is worth pointing out this factor as a possible contributor to the spread of data.

11.3 *Extrapolation of S/I vs Time Delay Curves*

In the example used to illustrate the calculation of single-echo intermodulation, the peak of the S/I versus time delay curve (Fig. 11) was

quite pronounced. This example assumed a path length of 200 miles and an rms deviation ratio of unity. For longer paths and higher deviation ratios, it is sometimes found that the highest value of S/I which can be calculated falls on the 6-db echo amplitude curve. This indicates that the peak of the curve may be further to the left of the 6-db contour, or in the region where the intermodulation theory of Ref. 4 is not valid. Although we have taken the liberty of extrapolating into this region to obtain certain of the values used in Figs. 13 to 16, it is clear that this is another source of possible error.

It is worth pointing out that in those cases where such extrapolation has been necessary to arrive at an estimate of intermodulation, the resulting value of S/I is poor enough to render the system rather useless. In a sense, then, the fact that there may be an error due to the extrapolation is academic.

XII. EFFECT OF DIVERSITY ON INTERMODULATION

The calculated results have been compared here to the S/I ratios measured without diversity. No approach has been found to date which permits analytical prediction of the diversity improvement; however, experimental results give some indication of the advantage to be expected.

Measurements of S/I were made with dual and quadruple diversity reception as well as without diversity on Paths 2, 3, and 4, and with dual diversity and nondiversity on Path 1. Generally, the difference in S/I between nondiversity and dual, and between dual diversity and quadruple, was 2 to 5 db. On the three Arctic paths, though, it is questionable whether the full advantage of diversity was being realized because the combiners were not working as well as expected, and there was some unexpected interference from testing equipment.

Dual diversity results for Path 1 showed an improvement in intermodulation over nondiversity during high deviations, but the nondiversity results were about equal to dual diversity results for low deviations.

To generalize, on the basis of measured data, one might expect to realize 3 or 4 db improvement in median S/I ratio with dual diversity over nondiversity reception, and another 3 or 4 db improvement for quadruple diversity over dual diversity.

XIII. SUMMARY OF ANALYTICAL-EMPIRICAL METHOD

The relatively good agreement between calculated and measured results indicates that the approach described in this paper is some progress

in the right direction. Further measurements and more accurate methods of measurement may show the way to refinements in the analysis which will improve its accuracy and minimize the present reliance on empirical adjustments.

There is given below a step-by-step summary of the method suggested for predicting the average intermodulation due to the propagation medium in a tropospheric scatter system. While the sequence is rather long and involved, many of the steps can be formulated in graphical or chart form for general use in a variety of cases. In fact, a computer program has been developed to accomplish steps 2 through 11, using as inputs the parameters listed in step 1.

The steps involved in the method are as follows:

1. Determine these parameters of the system and the path:
   a) Path length, statute miles
   b) Antenna beam pattern for the appropriate antenna size and operating frequency
   c) Antenna site elevation, feet, at each end
   d) Antenna take-off angles, θ_{t1} and θ_{t2}
   e) Minimum monthly median values of radio refractivity at sea level, N_o, in the areas of the two antenna terminals. (From Fig. 2.)
2. Calculate the surface values of refractivity, N_s, using (3) and the values of N_o found in step 1(e).
3. From Fig. 3, determine the values of the earth radius factor K corresponding to the values of N_s found in step 2. Estimate an average value of K for the path.
4. Compute the base angle, θ, defined by Fig. 1 and (2).
5. Compute the correction angle β, (4), to account for the difference in antenna site altitudes.
6. Compute the total angles θ_1 and θ_2 between the chord joining the antenna sites and the centerlines of the respective antenna beams, using (5) and (6).
7. Choose arbitrarily four or five values of reflection loss, r_e, spaced through the range of approximately 5 to 30 db.
8. Compute the value of ρ corresponding to each value of reflection loss selected in step 7, using (7).
9. Determine the additional loss of the echo path due to the antenna patterns, for each echo selected in step 7. Use (10) and (11) to determine the echo angles, and the antenna patterns of Fig. 8 to determine the reduction of gain at those angles.
10. Calculate the total loss for each echo, using (9).
11. Compute the time delay, T, for each echo, using (12).

12. For given base bandwidth and frequency deviation, use Fig. 9 to determine the value of S/I for each echo. (For a straight-FM system, use Figure 5.7 in Ref. 4.)
13. Plot S/I versus time delay for each echo, and determine the minimum value of S/I. Alternatively, the minimum can usually be estimated with sufficient accuracy from inspection of the calculated S/I values for the several echoes.
14. To account for multiple echoes, subtract 9 db from the minimum value of S/I found in Step 13.

The result of step 14 is the predicted value of the monthly mean S/I ratio during worst-month propagation conditions. The result applies to the top channel of a pre-emphasized FM system operating without diversity. For dual or quadruple diversity systems, add 3 db or 6 db, respectively. For other than worst-month propagation, add 0.7 db to the S/I ratio for each one-db decrease in path loss. (The correction factor may be slightly higher or lower than 0.7 db for a specific path, and should of course be modified appropriately if the S/I versus path loss function has been measured.)

The geometry of some paths may present unusual propagation characteristics calling for special treatment beyond the steps outlined above. The case of the 440-mile path discussed earlier is an example; on this path, it appeared that reflections from the tropopause may have contributed significantly to the intermodulation in the system. The implication of this case is that propagation anomalies can be expected on paths several hundred miles long, where the common volume extends to very high altitudes.

XIV. ACKNOWLEDGMENTS

The authors wish to express appreciation to P. V. Dimock for his leadership and encouragement in this work. They are indebted also to C. E. Clutts and W. A. Strong for many stimulating discussions and critical comment during the course of the study and in preparation of this paper. H. E. Curtis and S. O. Rice provided invaluable advice and consultation on the theory of intermodulation in FM systems, and A. B. Crawford and D. C. Hogg gave similar help on the theories underlying tropospheric scatter propagation. Thanks are due to Mrs. P. E. Collins, who performed many of the computations reported here, and to those who participated in the test program from which the experimental data were taken. The latter are too numerous to be cited individually.

APPENDIX A

Effect of Refractivity on Effective Earth Radius

We shall outline here a method for determining the approximate value of the effective earth's radius factor, K, applicable to a selected tropospheric scatter path.

K is expressed with sufficient accuracy for our purpose by[5]

$$K = \frac{R}{R_o} = \frac{1}{1 + \frac{dn}{dh} R_o} \tag{14}$$

where dn/dh is the vertical gradient of refractive index, n. In turn, define refractivity:

$$N = (n - 1)10^6. \tag{15}$$

Within a kilometer of the earth's surface,

$$\frac{dn}{dh} \approx \frac{\Delta N}{h} (10^{-6}) \tag{16}$$

where

$$\Delta N = N_h - N_s . \tag{17}$$

N_s is the refractivity at the surface, and N_h is the value at altitude h. When $h = 1$ km, it has been found from extensive data[5] that

$$\Delta N_{1\,\mathrm{km}} = -7.32 \exp (0.005577\, N_s). \tag{18}$$

One useful model of the atmosphere assumes an exponential decrease in N with altitude. Then:

$$N = N_s \exp (-Ch) \tag{19}$$

where h is altitude in kilometers above the ground. To fit the data quoted above, at $h = 1$ km,

$$C = \ln \frac{N_s}{N_s + \Delta N_{1\,\mathrm{km}}}. \tag{20}$$

Considering dn/dh to be constant with altitude (a good approximation only for the first 4000 or 5000 feet, but used here throughout because it introduces no appreciable error in calculating K for even the longest

path considered) and approximating it by the change in refractivity for the first 1000 feet only,

$$\frac{\Delta N}{1000 \text{ ft.}} = \frac{-N_s}{1000} [1 - \exp(-0.305\ C)]. \tag{21}$$

Substituting (16), (18), (20) and (21) in (14), K is found to be a function of N_s. This is plotted in Fig. 3.

Since the quantity to be calculated later is intermodulation during worst-month conditions, the K of interest is the value for the worst month. Maximum intermodulation generally corresponds to the minimum value of K, since it will produce least bending and hence longest echo delays. Minimum K corresponds to minimum N_s. N_s may be calculated from N_o, the sea level value of N, by

$$N_s = N_o \exp(-0.0322\ h) \tag{22}$$

where h here is the station altitude in thousands of feet. Minimum values of monthly mean N_o are given in Fig. 2, based on data collected from 306 weather stations over a period of several years.[6]

APPENDIX B

Calculation of Echo Amplitude Relative to Main Signal Amplitude

The technique involved here to calculate the magnitude of transmission echoes in a tropospheric scatter path makes use of (1) for received power. It will be convenient and helpful in this derivation to refer also to Fig. 6, which shows symmetrical main signal and echo paths having equal beamwidths α and α_e, respectively, and directed at angles θ and θ_e, respectively.

Equation (1) can be used to calculate the relative power received from the two paths, assuming the antenna gains in the directions θ and θ_e to be equal. (The effect of differences in antenna gain at θ and θ_e is discussed in the main text.) Expressing the ratio of the power of the main signal to the power of the echo by r', we have, from equation (1),

$$r' = \frac{P_r}{P_{re}} = \frac{\theta_e^5 \left(2 + \frac{\alpha_e}{\theta_e}\right) f\left(\frac{\alpha}{\theta}\right)}{\theta^5 \left(2 + \frac{\alpha}{\theta}\right) f\left(\frac{\alpha_e}{\theta_e}\right)}. \tag{23}$$

Setting $\alpha_e = \alpha$ and letting $\alpha \to 0$, the limit, r_e, will be the ratio between the power of a signal component traveling the centerline path and an echo traveling some longer path defined by θ_e.

Let $f(\alpha/\theta)$ be written as

$$g(\theta,\alpha) = \left[1 + \frac{\theta^4}{(\theta+\alpha)^4} - \frac{(2\theta+\alpha)^4}{8(\theta+\alpha)^4}\right]. \tag{24}$$

Then

$$\lim_{\alpha\to 0} r' = r_e = \frac{\theta_e^5}{\theta^5} \lim_{\alpha\to 0} \frac{g(\theta,\alpha)}{g(\theta_e,\alpha)}. \tag{25}$$

The above limit is undefined, and so is

$$\lim_{\alpha\to 0} \frac{g'(\theta,\alpha)}{g'(\theta_e,\alpha)}, \tag{26}$$

where $g' = dg/d\alpha$. Using L' Hospital's rule with the second derivative,

$$\lim_{\alpha\to 0} \frac{g''(\theta,\alpha)}{g''(\theta_e,\alpha)} = \left(\frac{\theta_e}{\theta}\right)^2 \tag{27}$$

or,

$$r_e = \left(\frac{\theta_e}{\theta}\right)^7 = (\rho)^7. \tag{28}$$

r_e will be called the "reflection loss" of an echo relative to the main signal.

APPENDIX C

Calculation of Echo Time Delay

The time delay of an echo which travels the path defined by θ_{1e}, θ_{2e} instead of the path θ_1, θ_2 (Fig. 7) is

$$T = \frac{\Delta L}{3(10)^8} \text{ seconds}, \tag{29}$$

where

$$\Delta L = (L_{1e} + L_{2e}) - (L_1 + L_2) \text{ meters}. \tag{30}$$

By the law of sines,

$$\begin{aligned}\Delta L &= \frac{2a\,(\sin\theta_{1e} + \sin\theta_{2e})}{\sin\,(\theta_{1e} + \theta_{2e})} - \frac{2a\,(\sin\theta_1 + \sin\theta_2)}{\sin\,(\theta_1 + \theta_2)} \\ &= \frac{2a\,(\sin\theta_{1e} + \sin\theta_{2e})}{\sin\theta_{1e}\cos\theta_{2e} + \sin\theta_{2e}\cos\theta_{1e}} \\ &\quad - \frac{2a\,(\sin\theta_1 + \sin\theta_2)}{\sin\theta_1\cos\theta_2 + \sin\theta_2\cos\theta_1}.\end{aligned} \tag{31}$$

For angles θ less than 0.1 radian* the following approximations are valid, applied to the above equation:

$$\cos \theta = 1 - \frac{\theta^2}{2}$$

$$\sin \theta = \theta$$

$$\frac{1}{1 - \frac{\theta_1\theta_2}{2}} = 1 + \frac{\theta_1\theta_2}{2}$$

$$2a = L.$$

Then

$$\Delta L = \frac{L}{2} (\theta_{1e}\theta_{2e} - \theta_1\theta_2) \text{ meters.} \tag{32}$$

Finally, for L in statute miles,

$$T = 2.68L\ \theta_1\theta_2(\rho^2 - 1) \text{ microseconds} \tag{33}$$

where

$$\rho = \frac{\theta_{1e}}{\theta_1} = \frac{\theta_{2e}}{\theta_2}.$$

REFERENCES

1. Booker, H. G., and Gordon, W. E., A Theory of Radio Scattering in the Troposphere, Proc. I.R.E., **38,** April, 1950, p. 401.
2. Villars, F., and Weisskopf, V. F., Scattering of EM Waves by Turbulent Atmospheric Fluctuations, Phys. Rev., **94,** April, 1954, p. 232.
3. Friis, H. T., Crawford, A. B., and Hogg, D. C., A Reflection Theory for Propagation Beyond the Horizon, B.S.T.J., **36,** May, 1957, p. 627.
4. Bennett, W. R., Curtis, H. E., and Rice, S. O., Interchannel Interference in FM and PM Systems Under Noise Loading Conditions, B.S.T.J., **34,** May, 1955, p. 601.
5. Bean, B. R., and Thayer, G. D., Models of the Atmospheric Refractive Index, Proc. I.R.E., **47,** May, 1959, p. 740.
6. Bean, B. R., and Horn, J. D., Radio-Refractive-Index Climate Near the Ground, Journal of Research of the Nat. Bur. of Standards D. Radio Propagation, Vol. **63D,** Nov.–Dec., 1959.
7. Clutts, C. E., Kennedy, R. N., and Trecker, J. M., Results of Bandwidth Tests on the 185-Mile Florida-Cuba Tropospheric Scatter Radio System, I.R.E. Trans. on Comm. Systems, Vol. **CS-9,** Dec., 1961, p. 434.

* Corresponds to path lengths less than about 800 miles. Paths of practical interest are appreciably shorter, and angles θ correspondingly smaller.